The Astronomical Journal, 151:54 (14pp), 2016 March doi:10.3847/0004-6256/151/3/54

QUASI-PERIODICITIES AT YEAR-LIKE TIMESCALES IN BLAZARS

A. Sandrinelli[1,2], S. Covino[2], M. Dotti[3,4], and A. Treves[1,2,5,6]
[1] Università degli Studi dell'Insubria, Dipartimento di Scienza ed Alta Tecnologia, Via Valleggio 11, I-22100 Como, Italy
[2] INAF—Istituto Nazionale di Astrofisica, Osservatorio Astronomico di Brera, Via Emilio Bianchi 46, I-23807 Merate, Italy
[3] Università degli Studi di Milano Bicocca, Dipartimento di Fisica G. Occhialini, Piazza della Scienza 3, I-20126 Milano, Italy
[4] INFN—Istituto Nazionale di Fisica Nucleare, Università degli Studi di Milano Bicocca, Dipartimento di Fisica G. Occhialini, Piazza della Scienza 3, I-20126 Milano, Italy
[5] INFN—Istituto Nazionale di Fisica Nucleare, Sezione Trieste—Udine, Via Valerio 2, I-34127 Trieste, Italy
Received 2015 June 2; accepted 2015 December 12; published 2016 February 9

ABSTRACT

We searched for quasi-periodicities on year-like timescales in the light curves of six blazars in the optical—near-infrared bands and we made a comparison with the high energy emission. We obtained optical/NIR light curves from Rapid Eye Mounting photometry plus archival Small & Moderate Aperture Research Telescope System data and we accessed the *Fermi* light curves for the γ-ray data. The periodograms often show strong peaks in the optical and γ-ray bands, which in some cases may be inter-related. The significance of the revealed peaks is then discussed, taking into account that the noise is frequency dependent. Quasi-periodicities on a year-like timescale appear to occur often in blazars. No straightforward model describing these possible periodicities is yet available, but some plausible interpretations for the physical mechanisms causing periodic variabilities of these sources are examined.

Key words: BL Lacertae objects: general – BL Lacertae objects: individual (PKS 0537–441, OJ 287, 3C 379, PKS 1510–089, PKS 2005–489), (PKS 2155–304) – galaxies: active – galaxies: statistics – galaxies: photometry

Supporting material: machine-readable table

1. INTRODUCTION

Blazars are active galactic nuclei exhibiting large variability at all frequencies. Their emission is dominated by a relativistic jet, the amplification factor of the intensity is characterized by a power of the Doppler factor (e.g., Ghisellini 2013). The jet produces a non-thermal spectrum where often one can distinguish a synchrotron and a Compton component. The energy source is assumed to be a combination of accretion on a supermassive black hole (SMBH) and extraction of its spin energy. In some cases the presence of an accretion disk is suggested by the appearance in the spectral energy distribution of a thermal component. The observed variability is supposedly a consequence of the intrinsic change of the accretion onto the SMBH, of the jet formation process, and specifically of its beaming. Various processes originating in different regions and with different timescales result in a complicated variability leading to rather chaotic light curves.

The study of variability through auto- and cross-correlation procedures has proven to be effective in constraining complex models of these sources. The discovery of a periodicity in the variability could have profound consequences in the global understanding of the sources, constituting a basic block for models. The effort for finding periodicities has been substantial at all frequencies (see, e.g., Falomo et al. 2014). A rather robust claim is that of a ∼12 year period in OJ 287 (e.g., Sillanpää et al. 1988), a BL Lac object possibly containing in its center a system of two SMBHs (Lehto & Valtonen 1996). Note, however, that the periodicity and the picture are disputed, for instance, by Hudec et al. (2013). Graham et al. (2015) proposed a 1980 day optical period for the quasar PG1302–102, which also appears reliable. Models based on the presence of a binary black hole (e.g., Sundelius et al. 1997; Kidger 2000; Valtonen & Ciprini 2012), describe outbursts and flares following a not strictly periodic cadence. In these cases, convolution of various processes can lead to an apparently unstable or variable period, i.e., to quasi-periodicities. Searching for quasi-periodicities in blazars is a valid and efficient diagnostic tool. Some sources could exhibit long lasting quasi-periodic behaviors. The timescales of the events and their persistence in the light curves may allow us to shed light on the physical processes underlying these variations. Among previous proposals of year-like quasi-periodicities in blazars, we refer to Raiteri et al. (2001), Kartaltepe & Balonek (2007), Gabányi et al. (2007), Rani et al. (2009), Li et al. (2015), and references therein. In addition, recently Zhang et al. (2014), collecting photometric data of PKS 2155–304 published in the last 35 years, discovered a quasi-periodicity of $T_0 = 317$ days. This was confirmed by our independent photometry (Sandrinelli et al. 2014a, 2014b). Moreover we showed that a periodicity appears also in the γ-rays observed by the *Fermi* mission at $T = 2 \cdot T_0$.

Because *Fermi* has continuously monitored the sky for ∼6 years, it is obvious that it is only now that one can combine optical and γ-ray searches for year-like periodicities, a procedure which was successful for PKS 2155–304. Since the number of covered periods in the optical and in γ-rays is limited, as in the case of PKS 2155–304, it is difficult to assess the stability on a long-term basis of the inferred (quasi) periodicities.

The starting point of the present investigation is the VRIJHK photometric observations obtained with the robotic Rapid Eye Mounting telescope (REM,[7] Covino et al. 2004; Zerbi et al. 2004) at La Silla, which are described in detail in Sandrinelli et al. (2014a). Among the blazar sources monitored by REM and described in the above mentioned paper we consider here

[6] ICRA.

[7] REM data can be retrieved from http://www.rem.inaf.it.

Table 1
Blazar Sample

Source	R.A.[a]	decl.[a]	Class[b]	SED[c]	Redshift[a]
PKS 0537–441	05:38:50	−44:05:09	BL Lac	LSP	0.896
OJ 287	08:54:48	+20:06:30	BL Lac	LSP	0.3060
3C 279	12:56:11	−05:47:21	FSRQ	LSP	0.536
PKS 1510–089	15:12:50	−09:05:59	FSRQ	LSP	0.3599
PKS 2005–489	20:09:25	−48:49:53	BL Lac	HSP	0.071
PKS 2155–304	21:58:52	−30:13:32	BL Lac	HSP	0.117

Notes.
[a] From the Simbad archive (http://simbad.u-strasbg.fr/).
[b] From Massaro et al. (2015).
[c] LSP, ISP and HSP refer to low, intermediate and high synchrotron peaked blazars (Abdo et al. 2010).

PKS 0537–441, OJ 287, PKS 1510–089, PKS 2005–489 and PKS 2155–304, because of the extensive coverage of the observations. These data are available on-line.[8] We also add the REM photometry of 3C 279, which is unpublished thus far. We have then combined the REM data with those derived from the Small & Moderate Aperture Research Telescope System archives (SMARTS,[9] Bonning et al. 2012). The REM data on PKS 2155–304 were originally examined in Sandrinelli et al. (2014b) and are those which led us to confirm the results of Zhang et al. (2014). In Table 1 we report a summary of the characteristics of the six sources, of which two are flat spectrum radio quasars (FSRQs) and the others are BL Lac objects.

The unpublished photometry of 3C 279 is described in Section 2. The search for periodicities from both optical data and *Fermi* archives is presented in Section 3. Discussion of results with a possible picture for the interpretation of a ∼1 year quasi-periodicity in blazars is reported in Section 4 and conclusions are in Section 5.

2. REM PHOTOMETRY OF 3C 279

The analysis of the data follows closely the scheme described by Sandrinelli et al. (2014a). For the optical bands we used reference stars from González-Pérez et al. (2001), while for the NIR frames we referred to the Two Micron All Sky Survey Catalog (2MASS,[10] Skrutskie et al. 2006).

All images have been visually checked, eliminating those where the targets or the reference stars are close to the borders of the frame, and where obvious biases were present. In Table 2 we report our photometry of the source. Some overall properties are given in Table 3. Comparing the fractional variability amplitude $\sigma_{\rm rms}$ (e.g., Nandra et al. 1997; Edelson et al. 2002) with those of the other five objects, 3C 279 appears highly variable. The nightly averaged light curves in the six filters are reported in Figure 1.

3. SEARCH FOR PERIODICITIES IN THE TARGET SOURCES

The starting point of our analysis is the light curves obtained combining REM (2005–2012) and SMARTS photometry (2008–2014) in the V, R, J, and K bands; see Figures 2–6 for the cases of the R and K filters. Note that contrary to our REM data, SMARTS' photometry is taken at face value, as archived in the public website. *Fermi* data[11] are also reported in Figures 2–6 in the 100 MeV–300 GeV band. The procedures for constructing gamma-ray curves are complex but rather standardized,[12] and are fully described, e.g., in Abdo et al. (2010). Note that these curves are not corrected for background.

Table 2
REM Photometry of 3C 279

Filter	Time of Observation (MJD)	Average Magnitude (mag)	Magnitude Error (mag)
V	53467	15.61	0.05
V	53469	15.64	0.06
V	53474	15.40	0.06
V	53476	15.16	0.04
V	53492	15.80	0.05

(This table is available in its entirety in machine-readable form.)

Table 3
Properties of REM NIR-optical Light Curves of 3C 279

Filter	Mag. Range (mag)	Mean mag. (mag)	Median (mag)	Flux Range (mJy)	$\sigma_{\rm rms}$[a] (%)
V	13.15–16.83	15.13	15.14	0.73–21.77	72 ± 2
R	12.70–16.58	14.83	14.95	0.83–27.37	83 ± 2
I	12.13–15.93	14.27	14.32	1.08–35.68	86 ± 2
J	10.90–15.03	13.04	13.07	1.55–69.30	82 ± 1
H	10.08–14.24	12.20	12.18	2.13–97.74	82 ± 1
K	9.58–13.30	11.18	11.18	3.33–99.81	66 ± 1

Note.
[a] Fractional variability amplitude.

The search for (quasi) periodicities in the light curves of active galactic nuclei is notoriously an arduous problem, as it was pointed out in the seminal paper by Press (1978), who considered the X-ray light curve of 3C 273 and indicated a number of caveats, which should be taken into account, before assessing the reality of a periodicity. In our case four main points should be examined.

1. Our optical sampling is rather irregular, as usual in ground-based observations. On the other hand γ-ray light curves are essentially evenly spaced.
2. The light curves are affected by frequency dependent *red* noise.
3. The total duration $T_{\rm tot}$ of the monitoring is $\leqslant$9 years in the optical, and $\leqslant$6 years in gamma-rays, constraining the minimum frequency that can be searched for.
4. Flares or periods of high activity can affect the analysis, requiring a careful check of the results.

The problem of the presence of red noise in evaluating a periodogram has been discussed in detail in the case of X-ray

[8] Photometric nightly averaged data is tabled in http://vizier.cfa.harvard.edu/viz-bin/VizieR?-source=J/A+A/562/A79
[9] http://www.astro.yale.edu/smarts/glast/home.php
[10] http://www.ipac.caltech.edu/2mass/
[11] http://fermi.gsfc.nasa.gov/ssc/data/access/lat/msl_lc/
[12] The data have been analyzed by using the standard *Fermi* LAT ScienceTools software package, see http://fermi.gsfc.nasa.gov/ssc/data/analysis/documentation/Cicerone/

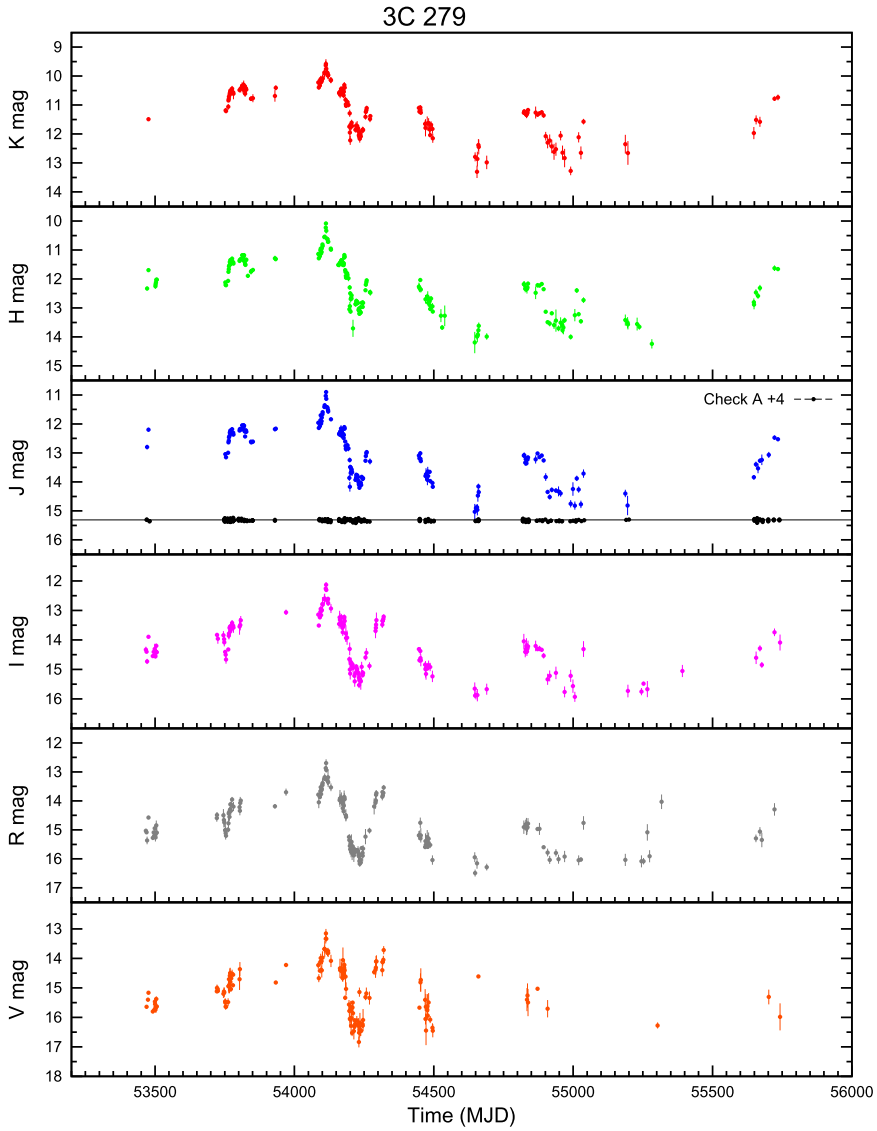

Figure 1. REM near-infrared and optical nightly averaged light curves of 3C 279. The light curve of the check star is reported in the J band (black points) with the indicated displacements Δm.

light curves, mainly in the context of galactic sources. The case of time series not being evenly spaced typically requires the use of interpolation techniques. Their application implies that the interpolated data points are no longer independent and may introduce a significant additional bias, which leads to an enhancement of low-frequency components at the expense of higher frequency ones (e.g., Schulz & Statteger 1997).

The assessment of the reality of periodicities cannot be carried out without firm procedures to measure a significance against the background noise. In particular the problem of the red noise modeling was examined by, i.e., Israel & Stella (1996), Vaughan (2005, 2010),van der Klis (1988), van der Klis (1989), Zhou & Sornette (2002), and Timmer & Koenig (1995), although usually for the simpler case of evenly sampled time-series.

A procedure for the study of periodicities in non-equally spaced light curves and affected by red noise was developed by Schulz & Mudelsee (2002) with reference to paleoclimatic time series.[13] In this procedure a first-order autoregressive (AR1) process is applied to model the red-noise (Hasselmann 1976). This avoids interpolation in the time domain with the introduced bias. The AR1 technique can give a good description of rather smooth and regular time-series, as is the case of the *Fermi* light curves we are considering here. Our optical light-curves are, on the contrary, much more difficult to model due to periods of high-activity and/or flares introducing orders of magnitude variations together with a highly irregular sampling. Nevertheless, the results of these analyses can provide useful hints about the significance of a detected possible periodicity, in particular when these periods are also present in the *Fermi* data.

We started with light curves with binning of 1 day in the optical bands, and 1 week in the γ-rays (see Figures 2–6). We considered γ-rays bins with test statistics (Mattox et al. 1996) TS > 4, corresponding to a $\sim 2\sigma$ detection. Note that for the large majority of cases the detections are much more significant than this limit. We have chosen a maximum frequency for the period analysis corresponding to $\sim$20 days. In fact, here we are not interested in the short

[13] Details on the relevant software "REDFIT" can be found at http://www.geo.uni-bremen.de/geomod/staff/mschulz/#software2.

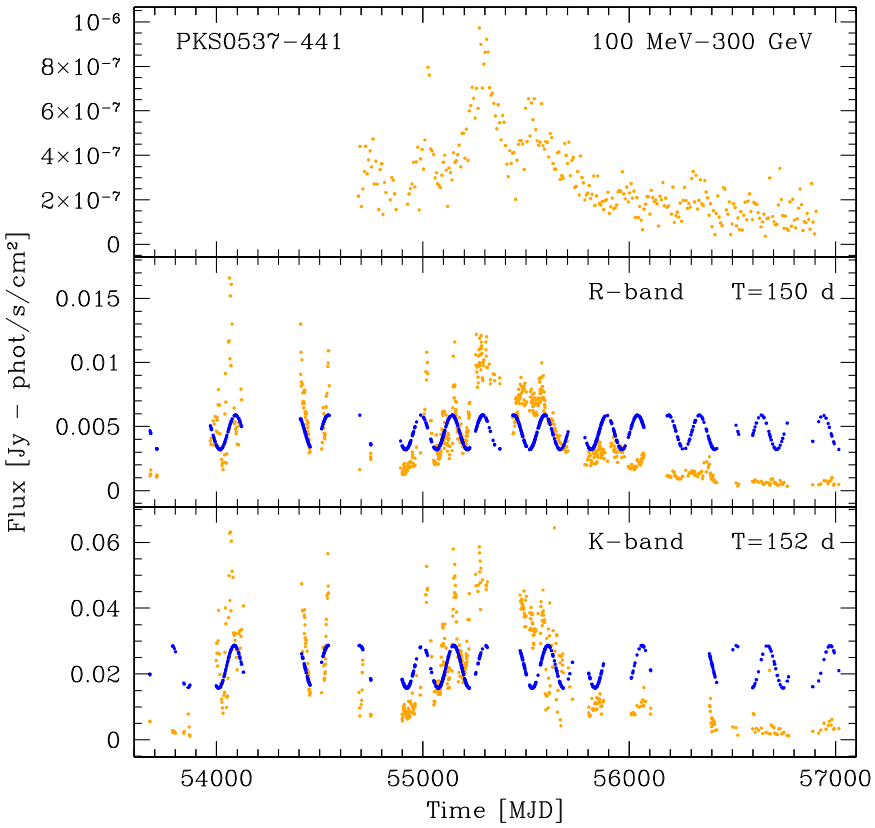

Figure 2. Weekly averaged *Fermi* γ-ray light curve in the 100 MeV–300 GeV energy range (top panel, yellow points). Nightly averaged REM and SMARTS light curves in R and K bands are also reported (central and bottom panels, yellow points). Flux is in photons s^{-1} cm^2 for the γ-ray light curve and in Jy for the NIR-optical light curves. Errors are omitted for readability. The blue lines are the sinusoidal artificial models (see the text). The amplitudes are $A = 0.001346$ Jy in R ($T = 150$ days), and $A = 0.00647$ Jy in the K band ($T = 152$ days).

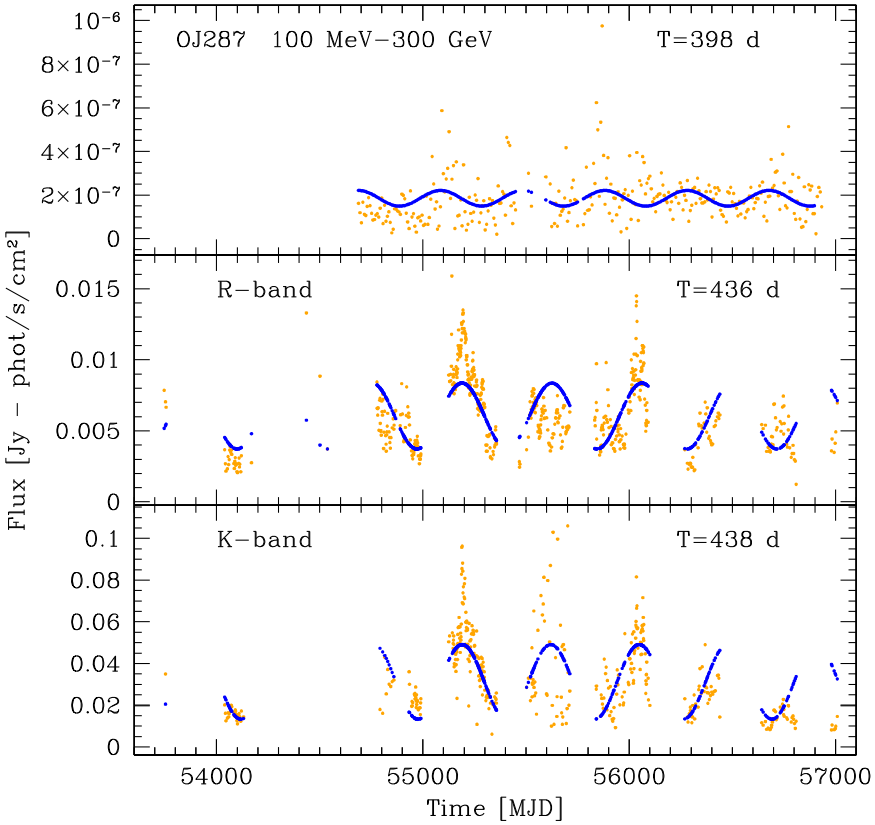

Figure 3. Same as Figure 2 for OJ 287. The amplitudes of the sinusoidal curves are $A = 3.60 \cdot 10^{-8}$ photons s^{-1} cm^2 in 100 MeV–300 GeV ($T = 398$ days), $A = 0.0023$ Jy in R ($T = 436$ days), and $A = 0.0179$ Jy in the K band ($T = 438$ days).

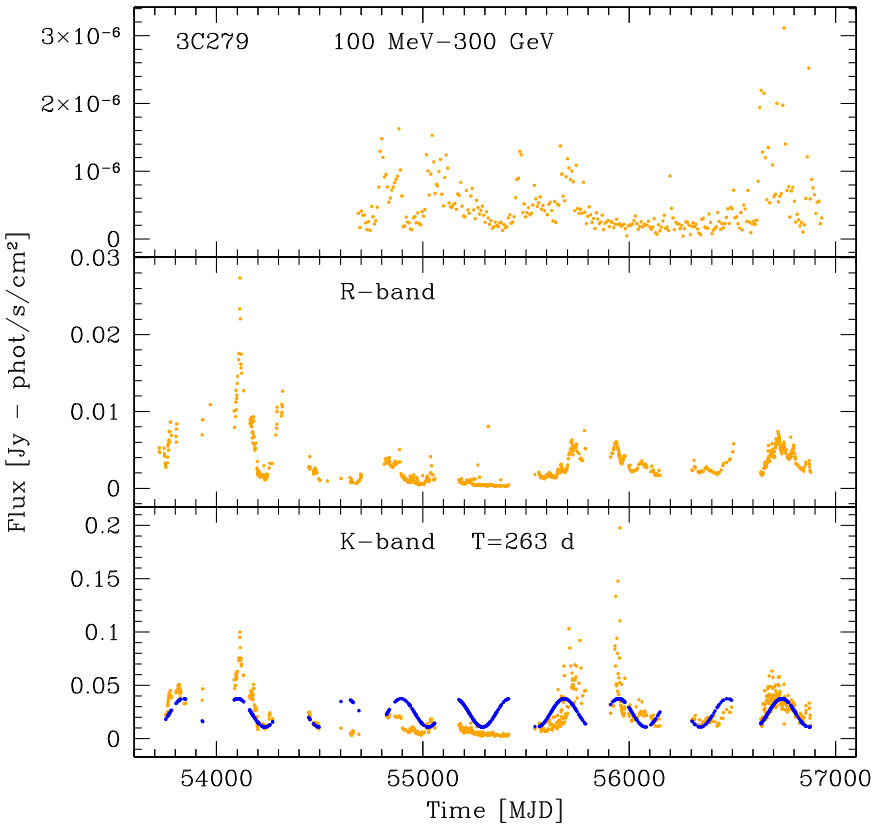

Figure 4. Same as Figure 2 for 3C 279. The amplitude A for the sinusoidal curve with a 263 day period in the K band is 0.0133 Jy.

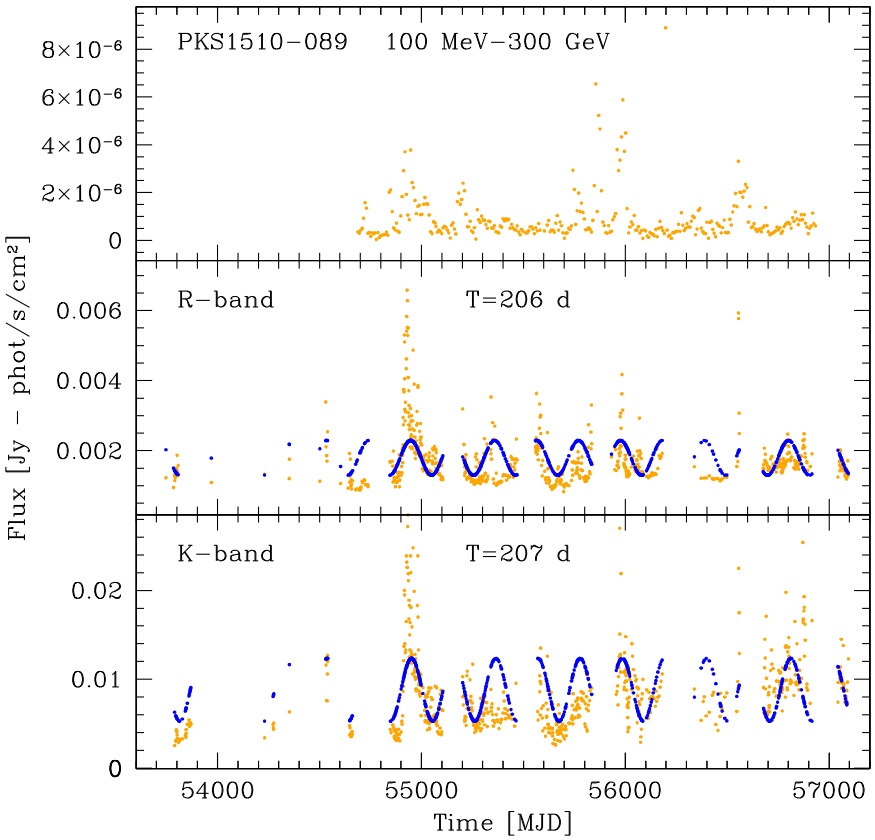

Figure 5. Same as Figure 2 for PKS 1510–089. The prominent flare occurring on ~54960 MJD is partially cut for an easier visualization of the data. Amplitudes of the sinusoidal curves are $A = 0.000497$ Jy in R ($T = 206$ days), and $A = 0.0048$ Jy in the K band ($T = 207$ days and $T = 474$ days).

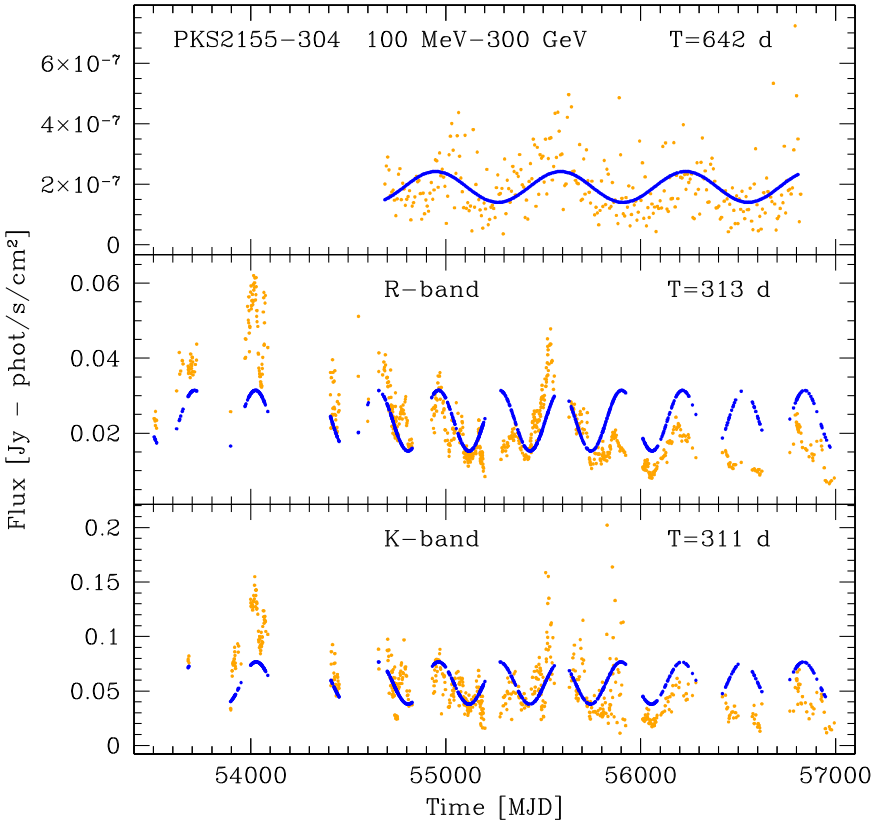

Figure 6. Same as Figure 2 for PKS 2155–304. Amplitudes of the sinusoidal curves are $A = 3.792 \cdot 10^{-7}$ photons s^{-1} cm^2 in 100 MeV–300 GeV ($T = 642$ days), $A = 0.00809$ Jy in R ($T = 313$ days), and $A = 0.0194$ Jy in the K band ($T = 311$ days).

Table 4
Most Prominent Peaks and Significances ($S \gtrsim 99\%$) in PKS 0537–441 *Observed* Power Spectra

Band	T_1 (days)	T_2 (days)	T_3 (days)	T_4 (days)	T_5 (days)	$S\% \gtrsim$
R	150 ± 5					99.0
		68 ± 1*				99.0
				61 ± 1*		99.0
					58 ± 1*	99.0
J	153 ± 3					99.0
		68 ± 1*				99.0
			64 ± 1*			99.0
				61 ± 1		99.7
					53 ± 1*	99.0
K	152 ± 4					98.0
		68 ± 1*				99.7
				61 ± 1		99.7
					53 ± 1*	99.7

Note. The peaks marked with (*) appear marginally revealed in our spectral analysis for Alias detection. We note that PKS 0537–441 is not observed by SMARTS in the V band.

Table 5
The Same as Table 4 for OJ 287

Band	T_1 (days)	T_2 (days)	T_3 (days)	$S\% \gtrsim$
100 MeV–300 Gev	412 ± 25			99.0
V	435 ± 24			99.7
R	436 ± 27			99.0
J	436 ± 25			99.7
		303 ± 12*		99.0
K	438 ± 22			99.7
		296 ± 10*		99.7
			203 ± 5	99.7

timescale variability. The procedure yields (see Figures 7–12):

1. Lomb and Scargle periodograms (Scargle 1982), which account for the unevenly spaced photometry.
2. Modeling of red noise continuum.
3. Bias-corrected spectra and significance (S) level curves: we have chosen $S = 99.0\%$ (2.5σ) and $S = 99.7\%$ (3σ).

The significance is given by the comparison of the periodogram with that based on the auto-regressive model (see above) to test the null hypothesis that the observed time series can be fully accounted for by the noise.

In Tables 4–9 we report the *observed* periods corresponding to peaks with $\gtrsim$99% significance. We evaluated the period uncertainty following Schwarzenberg-Czerny (1991), searching for the mean noise power level (MNPL) in the vicinity of the investigated period T. The 1σ confidence interval on T is the width of the peak in the power spectrum at p–MNPL, where

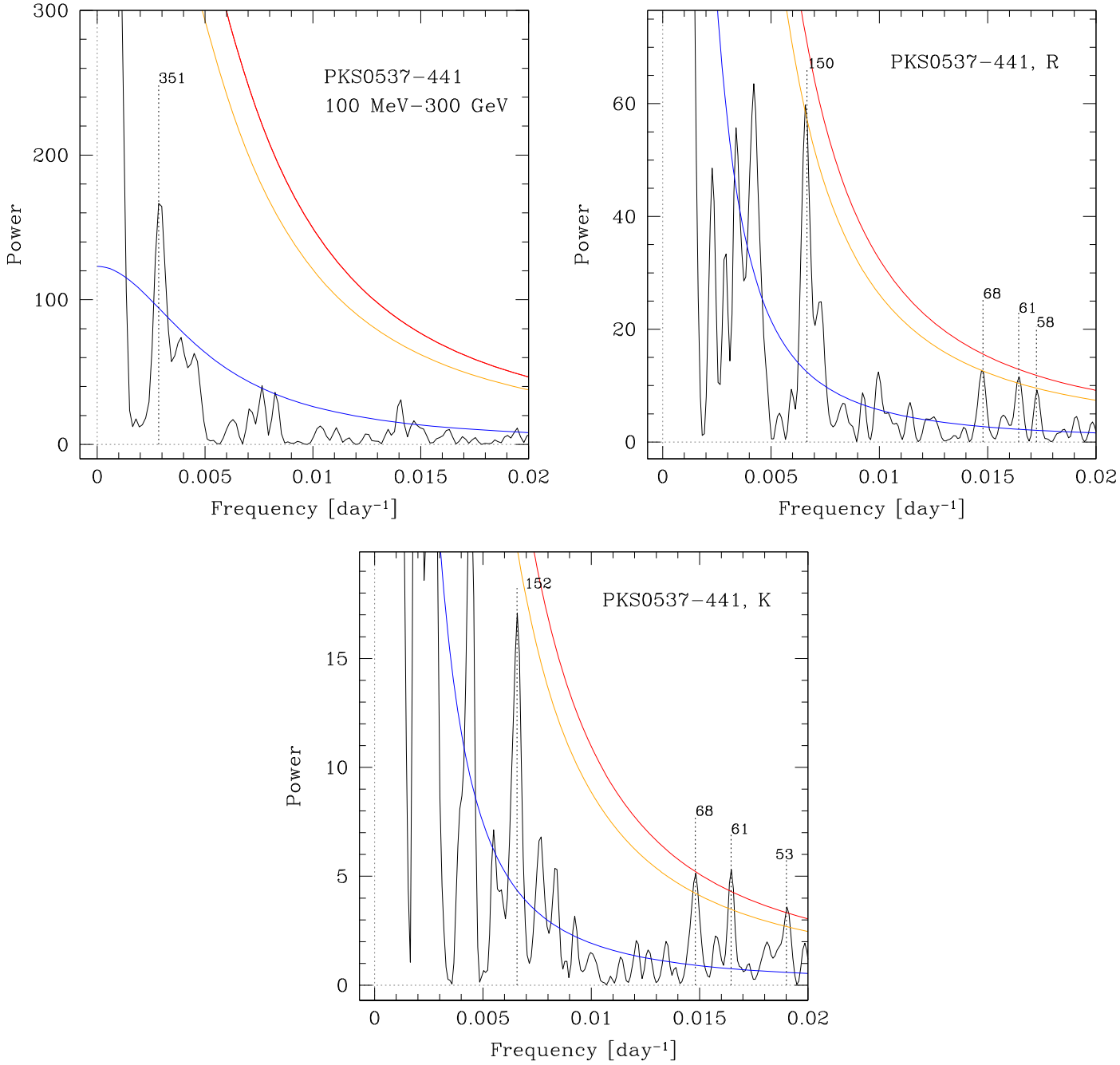

Figure 7. Bias-corrected power spectra (black line) of the blazar sample in 100 MeV–300 GeV from the *Fermi* γ-ray light curves, and in the K and R bands from REM + SMARTS photometry (see also Tables 4–9). The power is the output obtained by the procedure of Schulz & Mudelsee (2002, REDFIT) normalized with the variance. Curves in each panel, starting from the bottom, are: the theoretical red-noise spectrum, and the 99.0% (2.5σ) and 99.7% (3σ) χ^2 significance levels. Periods in days corresponding to the prominent peaks are marked.

p is the height of the peak. The sinusoidal artificial light-curves with the most significant periods calculated using Vstar package[14] are reported in Figures 2–6. We checked for aliases derived from the interval sampling between observations or the sampling rate, which cause false peaks in the time analysis (see e.g., Deeming 1975). We adopted the procedure in the Period Analysis Software[15] and found in all the NIR-optical curves evidence of an alias period of ∼370 days, which is representative of the year length. The corresponding peak is negligible with respect to the other periodicities in all the sources, with the exception of PKS 2005–489. Applying the same procedure to γ-ray light curves, no aliases have been detected, as expected, except for a significant one at 7 days, denoting the sampling rate of the *Fermi* data. The peaks, which appear marginally revealed in the spectral analysis for alias detection, are marked in Tables 4–9.

We now examine the sources separately, discussing the most important possible periodicities detected by the analysis. As a general point, several periods appear to have a formal

[14] http://www.aavso.org/vstar-overview
[15] http://www.peranso.com

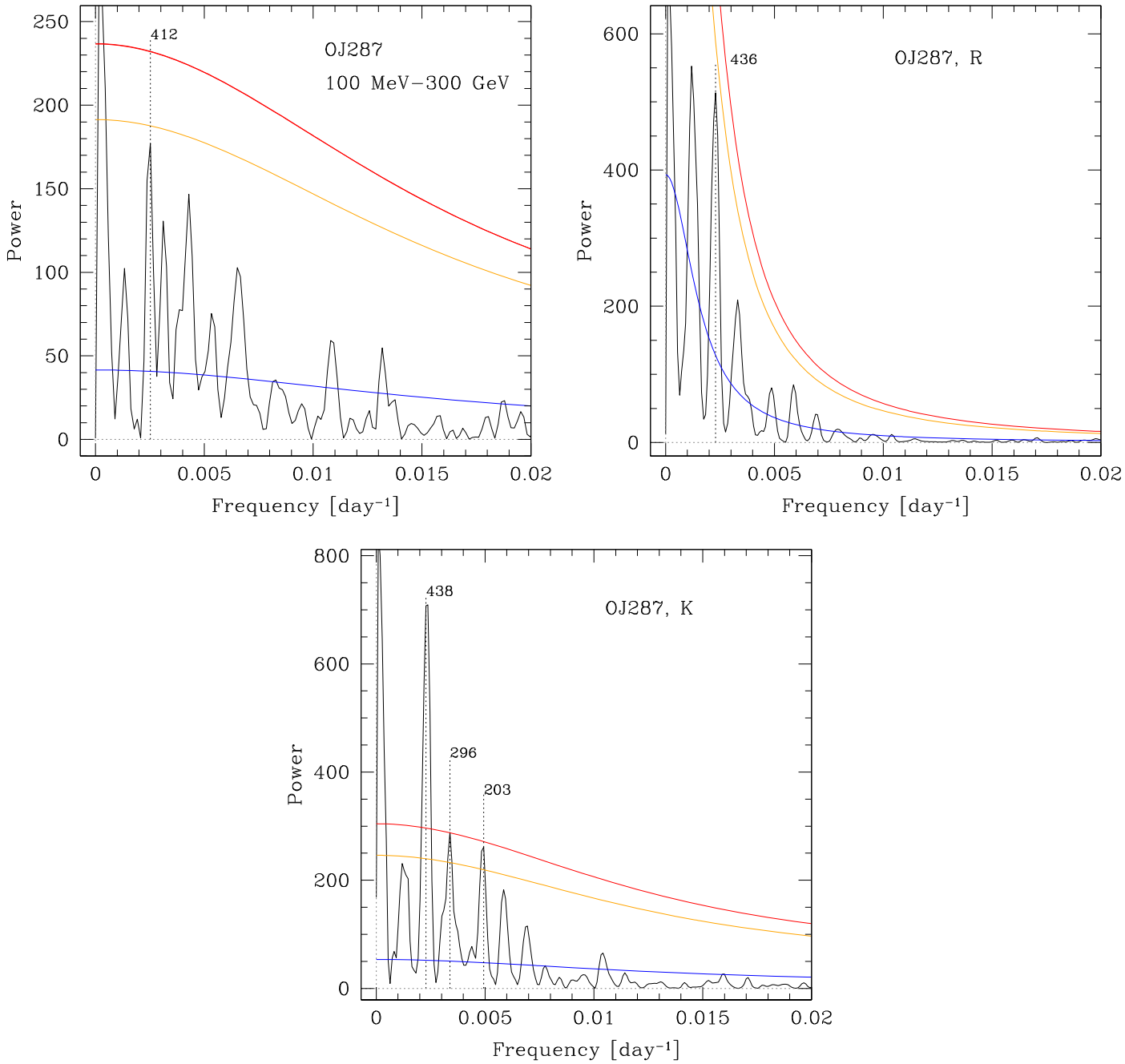

Figure 8. The same as Figure 7 for OJ 287.

significance close to or better than 99%. However, considering the many possible sources of uncertainty (mainly in the optical/NIR) it may be not sufficient to provide a fully solid statement about their reliability.

PKS 0537–441. In the R, J, and K bands there are peaks at $T_1 \sim 150$ days with a significance $S \gtrsim 98\%$, as reported in Table 4, and in the γ-rays a peak appears at 351 days with $S \sim 90\%$, see Figure 7. The most prominent peak at 1668 days is close to the total observing time $T_{\rm tot}$ and it is not reported in Table 4 and Figure 7.

OJ 287. In the NIR-optical bands plotted in Figure 3 there are peaks at $T_1 \sim 435$ days ($S \gtrsim 99.7\%$ in V, J, and K, see Table 5), which within the errors may be related to the γ-ray periodicity at ∼410 days ($S \sim 99\%$).

3C 279. As is apparent from Figure 4, there are significant peaks at $T_1 \sim 910$ days, which, however, are comparable with $T_{\rm tot}$. T_1 is the most prominent one, which can be taken into account at low frequencies in the γ-ray spectrum ($S \gtrsim 95\%$). It is noticeable that peaks at T_1 and $T_7 \sim 24$ days are present both in the periodograms of the γ-ray data and of the NIR-optical bands (in K band for T_1 S is <99.7%); see Figure 9 and Table 6. In the NIR-optical bands the presence of peaks at $T_2 \sim 260$ days, with significance $\geqslant 3\sigma$ in V and K, stands out. In the R and V bands the adopted procedure fails at producing a reliable red-noise profile due to the prominent flare at ∼MJD 53700. In this case the search for periodicities was performed by splitting the light curve in 3 segments, which are overlapping for the 50% of their lengths (Welch-overlapped-

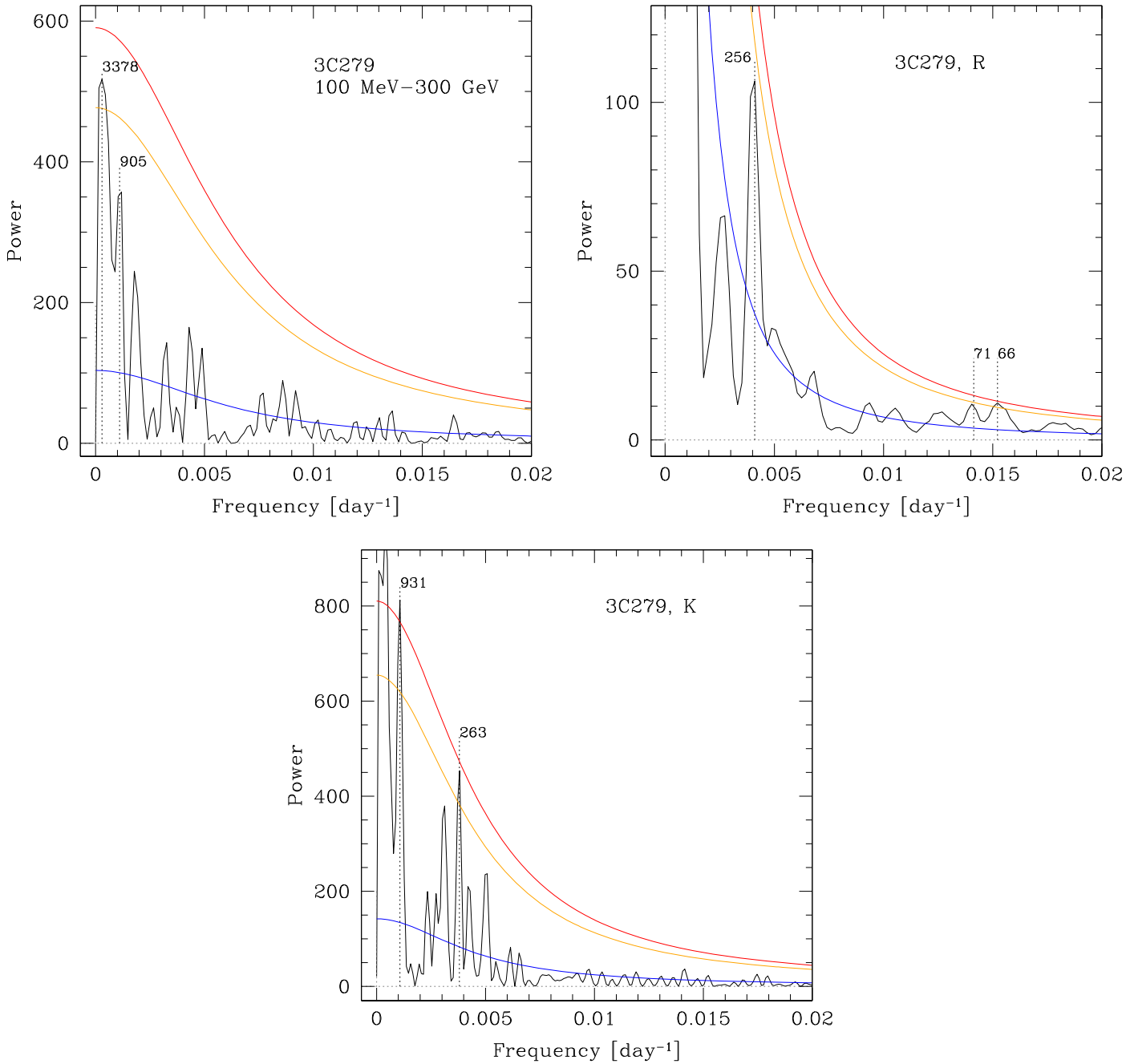

Figure 9. The same as Figure 7 for 3C 279.

segment-averaging, WOSA, Welch 1967). The spectral features are estimated from averaging the three resulting periodograms. The obtained spectra return peaks at 256 days, which we can associate with the one at ∼265 days in the K band (see Figure 9 and Table 6).

PKS 1510–089. The most significant peak in the γ-ray band is at $T_5 = 115$ days ($S \sim 99\%$); see Figure 10. This may be related to the optical peaks at $4 \cdot T_5$ and $3 \cdot T_5$, with $S > 99.0\%$ (see Table 7). We note that in this source the fit of the red noise continuum may be affected by a number of short flares (Sandrinelli et al. 2014a).

PKS 2005–489. For this source only REM photometry is available. A conspicuous peak at ∼680–720 days is present in all the NIR-optical bands (Figure 11 and Table 8). It may be related to the peak at ∼370 days, which, however, is supposedly spurious (see above). Because of the length of the light curve ($T_{\rm tot} = 2500$ days) the candidate periods between 1000 and 1500 days are hardly significant and are not reported in Table 8.

PKS 2155–304. We confirm the results presented in Sandrinelli et al. (2014b) about a peak of $T_3 \sim 315$ days in the NIR-optical bands and at $2 \cdot T_3$ in the γ-rays; see Table 9 and Figure 12. In γ-rays and in K the significances are above 3σ. In K the presence of peaks with $S \gtrsim 99\%$ at 453 and 151 days is also noticeable, which, with $2 \cdot T_3$ and T_3, could be harmonics of the same period $T_7 = 76$ days.

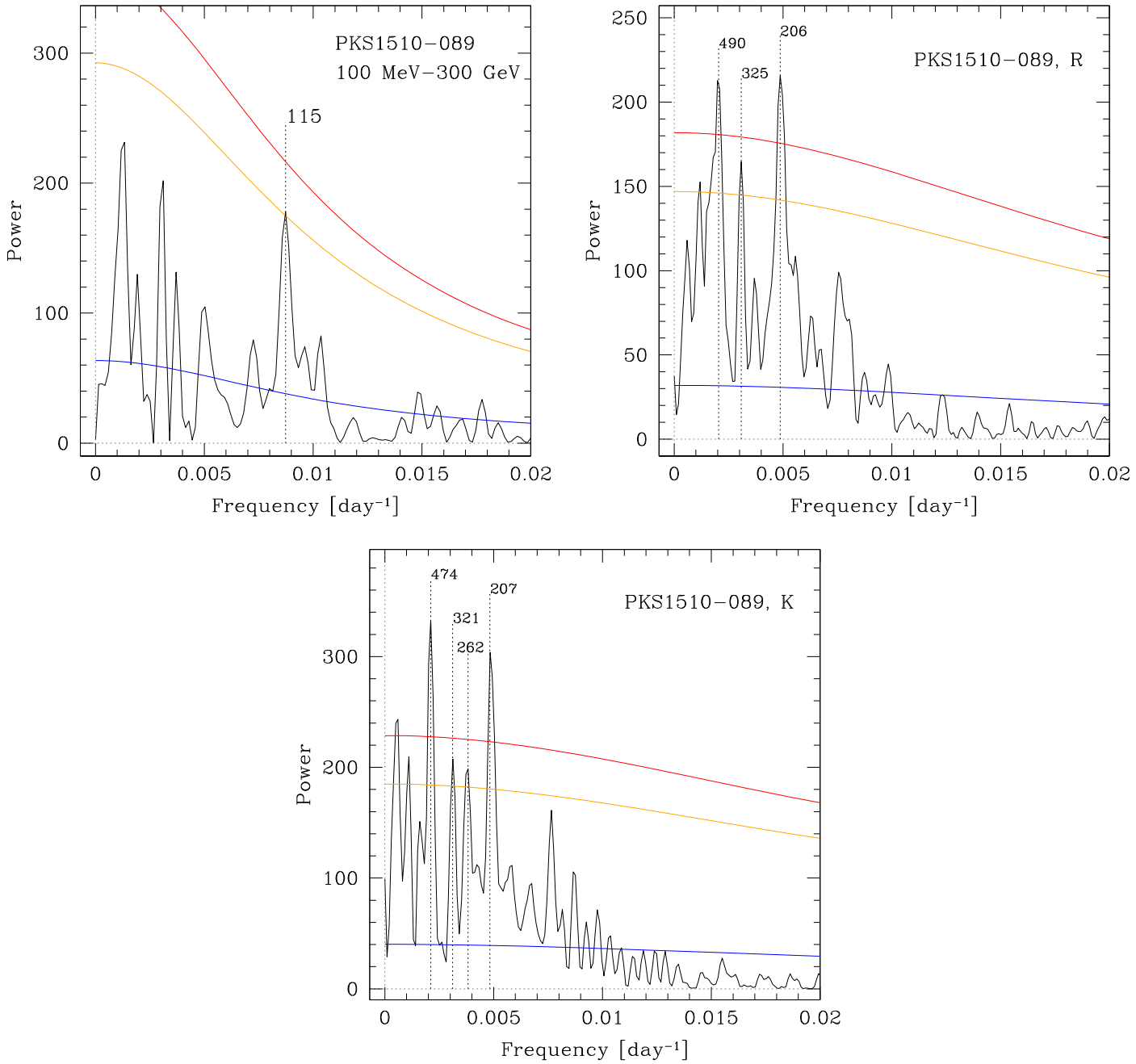

Figure 10. The same as Figure 7 for PKS 1510–089.

4. DISCUSSION

The advent of robotic telescopes in the last decade and the systematic monitoring of the γ-ray sky since 2008, gave an unprecedented opportunity for exploring quasi-periodicities in blazars at year-like timescales. The presence of possible associated periodicities in both the optical and γ-ray bands may be indicative of their physical relevance. The most convincing cases are PKS 2155–304, OJ 287, and 3C 279.

In the following we discuss some possible interpretations for the physical mechanisms causing the periodic variability of these sources with a rest-frame year-like duration. As already discussed in Sandrinelli et al. (2014b) and similar to the interpretation proposed by Lehto & Valtonen (1996) for OJ 287, the observed year-like timescale periodicity could be related to the orbit of a perturbing object. This could destabilize the accretion flow onto the primary SMBH, modulating the accretion rate, and as a consequence, the luminosity of the active nucleus. Assuming the mass of the active SMBH is $M_1 \sim 10^9 M_\odot$ (typical of blazars) and that the perturber is significantly less massive ($q = M_2/M_1 < 0.1$), the observed periodicity implies a separation between the two bodies of $d \sim 100\ r_S \approx 10^{-2}$ pc, where r_S is the Schwarzschild radius of the central SMBH. Currently available observations do not allow us to constrain the nature of the perturber. Even assuming that this is a secondary SMBH of mass $\sim 10^8 M_\odot$, the gravitational wave (GW) driven orbital decay would be of the order of 1 Myr (Peters 1964), making it hard to observe any frequency drift due to the shrinking of the perturber orbit.

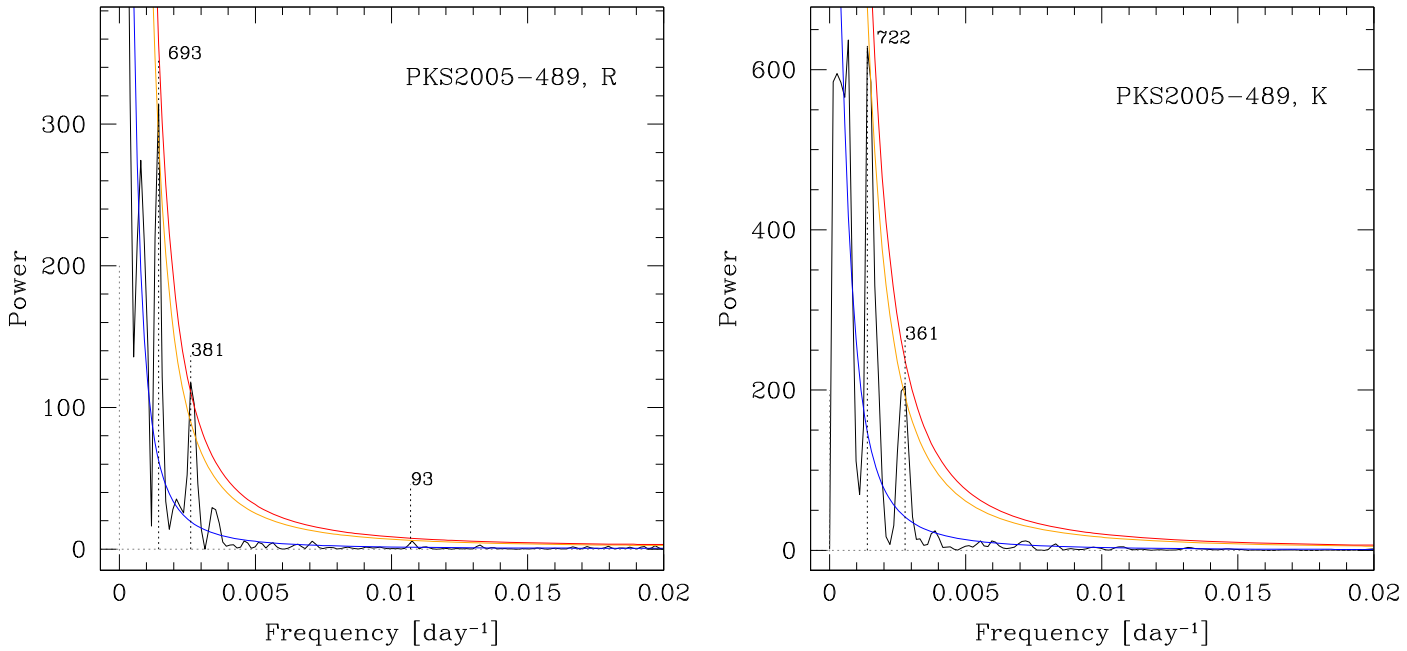

Figure 11. The same as Figure 7 for PKS 2005–489.

Table 6
The Same as Table 4 for 3C 279

Band	T_1 (days)	T_2 (days)	T_3 (days)	T_4 (days)	T_5 (days)	T_6 (days)	T_7 (days)	$S\%\gtrsim$
100 MeV–300 GeV					39 ± 1			99.7
							24 ± 1	99.7
V		256 ± 15						99.7
R		256 ± 12						99.0
			71 ± 1					99.0
				66 ± 1				99.0
						29 ± 1*		99.0
							24 ± 1	99.7
K	931 ± 46							99.7
		263 ± 5						99.7

Table 7
The Same as Table 4 for PKS 1510–089

Band	T_1 (days)	T_2 (days)	T_3 (days)	T_4 (days)	T_6 (days)	$S\%\gtrsim$
100 MeV–300 Gev					115 ± 5	99
V	490 ± 34					99.0
		325 ± 16				99.7
R	490 ± 37					99.7
		325 ± 13				99.0
				206 ± 9		99.7
J	474 ± 36					99.7
		321 ± 15				99.0
				203 ± 9		99.7
K	474 ± 34					99.7
		321 ± 16				99.0
			262 ± 10*			99.0
				207 ± 10		99.7

Table 8
The Same as Table 4 for PKS 2005–489

Band	T_1 (days)	T_2 (days)	T_3 (days)	$S\%\gtrsim$
V	719 ± 64*			97
		360 ± 44*		99
			93 ± 2*	99.7
R	693 ± 74*			99
		381 ± 48*		99.7
			93 ± 1*	99
J	683 ± 51*			99
		381 ± 39*		99.7
K	722 ± 47			99
		361 ± 28*		99

A second possibility is that the observed periodicity is related to the precession period of the blazar jet. We can draw two distinct scenarios, depending on whether the jet is forced to be aligned to the SMBH spin or not. In this second case the jet would be aligned to the angular momentum of the inner part of the accretion disc. In the case in which the inner disc is not lying on the SMBH equatorial plane, it would undergo Lense-Thirring precession around the SMBH spin. The Lense Thirring precession period scales as

$$T_{\rm Prec} = \frac{8\pi G M_1}{c^3 a}\left(\frac{r}{r_S}\right)^3, \quad (1)$$

where a is the SMBH spin parameter. If the accretion flow is geometrically thick, the inner disk precesses as a solid body, as demonstrated by general relativistic magnetohydrodynamic

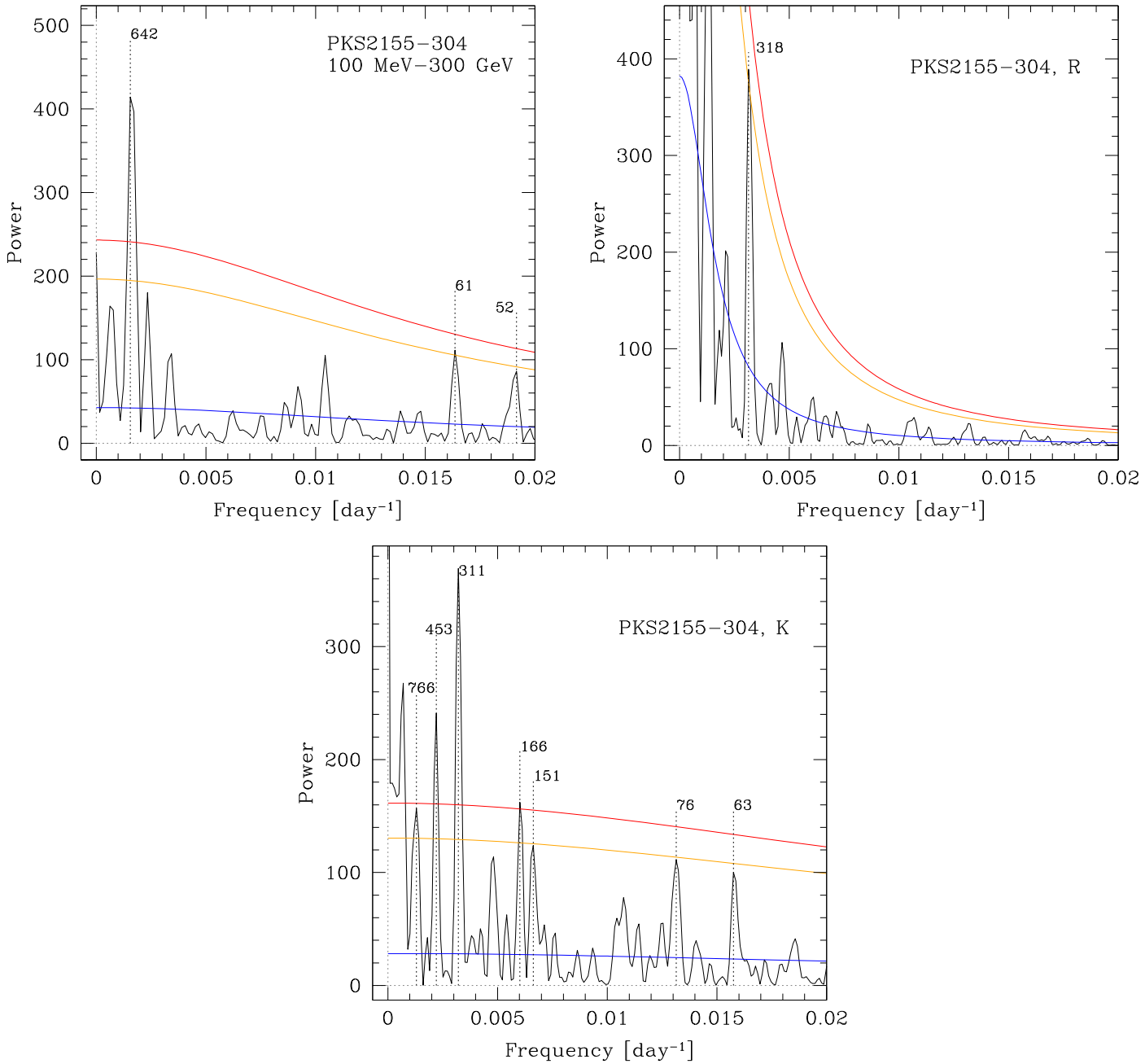

Figure 12. The same as Figure 7 for PKS 2155–304.

numerical simulations (e.g., Fragile et al. 2007; Dexter & Fragile 2011).[16] In this case the observed period does provide an estimate of the size of the inner precessing region. About 900 day correspond to $\approx 8 r_S$, while $\approx$300 day would imply $\approx 5 r_S$ (both the estimates assume $M_1 = 10^9 M_\odot$ and $a = 0.9$).

If instead the jet is aligned with the SMBH spin, the observed periodicity has to be related to the precession timescale of the spin itself. In order for the observed flux to be significantly affected by the precession, the angle between the SMBH spin and the axis of precession (defined by the total angular momentum of the system) has to be of the order of the jet opening angle $\sim 1^\circ$ or greater. Because of the large mass of the SMBH, the angular momentum of the accreting gas within the inner $\sim 10 r_S$ cannot cause such a large displacement of the SMBH spin. A secondary SMBH orbiting at $\approx 8 r_S$ is required in this case. The secondary mass needed to cause a significant variation in the observed flux has to be $M_2 \gtrsim 10^6 M_\odot$. This last scenario has a number of testable predictions:

(i) The lifetime of such a system would be determined by the GW driven orbital decay of the binary. The timescale is $\gtrsim 8 \cdot 10^3$ years for $M_2 \gtrsim 10^6 M_\odot$ and it scales with the inverse of M_2. For $M_2 \gtrsim 10^7 M_\odot$ a drift of the period toward smaller values could be observable in the next decades;

[16] We note that a thick geometry is expected for radiatively inefficient accretion, making this scenario particularly attractive for BL Lacs and specifically for PKS 2155–304 (Ghisellini et al. 2011; Sbarrato et al. 2012).

Table 9
The Same as Table 4 for PKS 2155–304

Band	T_1 (days)	T_2 (days)	T_3 (days)	T_4 (days)	T_5 (days)	T_6 (days)	T_7 (days)	T_8 (days)	T_9 (days)	$S\%\gtrsim$
100 MeV–300 GeV	642 ± 59									99.7
								61 ± 1*		99.0
									52 ± 1	99.0
V			318 ± 14							99.0
							75 ± 1			99.7
								64 ± 1*		99.0
R			318 ± 14							99.0
J			310 ± 15							99.0
							76 ± 1			99.0
								63 ± 1*		99.0
K		453 ± 16								99.7
			311 ± 14							99.7
				166 ± 2						99.7
					151 ± 2					99.7
						93 ± 1*				99.0
							76 ± 1			99.0

(ii) A faster variability, corresponding to the orbital timescale of the binary, could be observed (with a period of ≈24 days assuming $q < 0.1$).

In a different scenario, the detected quasi-periodic oscillations in blazars could be related to jet emissions. Variability can be ascribed to helical jets or helical structures in jets (e.g., Camenzind & Krockenberger 1992) which may be quite common in blazars (Villata & Raiteri 1999). They could arise from hydrodynamical instabilities in magnetized jets (Hardee & Rosen 1999) or from variations in the jet engine, e.g., accretion disk instabilities (Godfrey et al. 2012, and reference therein), also coupled with the interaction of the jet plasma with the surrounding medium. The emitting flow moving around a helical path could produce relatively long-term quasi-periodic changes in Doppler boosted flux (Villata & Raiteri 1999). In such a picture a rotating helical structure was proposed to explain, e.g., both the quasi-periodic behavior (∼8 years, Raiteri et al. 2010) of BL Lacertae and the occurrence and the mean shape of major radio-optical outbursts in AO 0235 +16 (∼5.7 years, Ostorero et al. 2004). Relativistic shocks (e.g., Marscher & Gear 1985) exciting jet helical patterns can also be considered (e.g., Rani et al. 2009; Larionov et al. 2013), as well as models based on dominant turbulent cells in a plasma jet (Marscher et al. 1992; Marscher 2014) driving short-lived quasi-periodic oscillations behind a shock (e.g., Rani et al. 2009). The presence of quasi-periodic peaks in radio-mapped jet emissions is, for instance, discussed in Godfrey et al. (2012) for the case of PKS 0637–752, where large-scale shocks in continuous flow are invoked (re-confinement shocks, Kelvin–Helmholtz instabilities). The discussion by Godfrey et al. (2012) proposes timescales of variability much larger than those inferred in this paper, but the issue should be reconsidered in detail.

5. CONCLUSIONS

The significance of the detected periods is almost never very high, although in several cases it is good enough to deserve consideration. As discussed in the text, a periodicity analysis of highly irregular and unevenly sampled time-series is never an easy task. On the other hand, in some cases the detected periods are also connected with periods derived from *Fermi* data, where most of the source of uncertainty do not apply. It is then possible that quasi-periodicities of ∼1 year in blazars are not rare. Their origin is not easy to be traced, and detailed models are not yet available.

Progress in the field can come from the study of other blazars, which have long optical monitoring, and are relatively bright in the *Fermi* archives. It is also obvious to search for confirmation of the periodicities in the X-rays where large amount of sparse observations are archived. However, the X-rays could be produced independently of the optical and γ-rays. For the future, observations of the SMARTS and REM type should hopefully be prosecuted for several years, largely improving the robustness of the analysis for periodicities of several months/one year length.

We are grateful to Dr. G.L. Israel for discussions on periodicity searches in light curves affected by red noise. This paper made use of up-to-date SMARTS optical/near-infrared light curves that are available online.[17] We acknowledge the support of the Italian Ministry of Education (grant PRIN-MIUR 2009, 2010, 2011). This work was also supported by ASI grant I/004/11/0.

REFERENCES

Abdo, A. A., Ackermann, M., Ajello, M., et al. 2010, ApJ, 722, 520
Bonning, E., Urry, C. M., Bailyn, C., et al. 2012, ApJ, 756, 13
Camenzind, M., & Krockenberger, M. 1992, A&A, 255, 59
Covino, S., Stefanon, M., Sciuto, G., et al. 2004, Proc. SPIE, 5492, 1613
Deeming, T. J. 1975, Ap&SS, 36, 137
Dexter, J., & Fragile, P. C. 2011, ApJ, 730, 36
Edelson, R., Turner, T. J., Pounds, K., et al. 2002, ApJ, 568, 610
Falomo, R., Pian, E., & Treves, A. 2014, A&ARv, 22, 73

[17] www.astro.yale.edu/smarts/glast/home.php

Fragile, P. C., Blaes, O. M., Anninos, P., & Salmonson, J. D. 2007, ApJ, 668, 417
Gabányi, K. É., Marchili, N., Krichbaum, T. P., et al. 2007, A&A, 470, 83
Ghisellini, G. 2013, Radiative Processes in High Energy Astrophysics (Berlin: Springer)
Ghisellini, G., Tavecchio, F., Foschini, L., & Ghirlanda, G. 2011, MNRAS, 414, 2674
Godfrey, L. E. H., Lovell, J. E. J., Burke-Spolaor, S., et al. 2012, ApJ, 758, L27
González-Pérez, J. N., Kidger, M. R., & Martín-Luis, F. 2001, AJ, 122, 2055
Graham, M. J., Djorgovski, S. G., Stern, D., et al. 2015, Natur, 518, 74
Hardee, P. E., & Rosen, A. 1999, ApJ, 524, 650
Hasselmann, K. 1976, Theory Tellus, 28, 473
Hudec, R., Bašta, M., Pihajoki, P., & Valtonen, M. 2013, A&A, 559, A20
Israel, G. L., & Stella, L. 1996, ApJ, 468, 369
Kartaltepe, J. S., & Balonek, T. J. 2007, AJ, 133, 2866
Kidger, M. R. 2000, AJ, 119, 2053
Larionov, V. M., Jorstad, S. G., Marscher, A. P., et al. 2013, ApJ, 768, 40
Lehto, H. J., & Valtonen, M. J. 1996, ApJ, 460, 207
Li, H. Z., Chen, L. E., Yi, T. F., et al. 2015, PASP, 127, 1
Marscher, A. P. 2014, ApJ, 780, 87
Marscher, A. P., & Gear, W. K. 1985, ApJ, 298, 114
Marscher, A. P., Gear, W. K., & Travis, J. P. 1992, in Variability of Blazars, ed. E. Valtaoja, & M. Valtonen (Cambridge: Cambridge Univ. Press), 85
Massaro, E., Giommi, P., Leto, C., et al. 2015, Ap&SS, 357, 75
Mattox, J. R., Bertsch, D. L., Chiang, J., et al. 1996, ApJ, 461, 396
Nandra, K., George, I. M., Mushotzky, R. F., Turner, T. J., & Yaqoob, T. 1997, ApJ, 476, 70
Ostorero, L., Villata, M., & Raiteri, C. M. 2004, A&A, 419, 913
Peters, P. C. 1964, PhRvB, 136, 1224
Press, W. H. 1978, ComAp, 7, 103
Raiteri, C. M., Villata, M., Aller, H. D., et al. 2001, A&A, 377, 396
Raiteri, C. M., Villata, M., Bruschini, L., et al. 2010, A&A, 524, A43
Rani, B., Wiita, P. J., & Gupta, A. C. 2009, ApJ, 696, 2170
Sandrinelli, A., Covino, S., & Treves, A. 2014a, A&A, 562, A79
Sandrinelli, A., Covino, S., & Treves, A. 2014b, ApJ, 793, L1
Sbarrato, T., Ghisellini, G., Maraschi, L., & Colpi, M. 2012, MNRAS, 421, 1764
Scargle, J. D. 1982, ApJ, 263, 835
Schulz, M., & Mudelsee, M. 2002, CG, 28, 421
Schulz, M., & Statteger, K. 1997, CG, 23, 929
Schwarzenberg-Czerny, A. 1991, MNRAS, 253, 198
Sillanpää, A., Haarala, S., Valtonen, M. J., Sundelius, B., & Byrd, G. G. 1988, ApJ, 325, 628
Skrutskie, M. F., Cutri, R. M., Stiening, R., et al. 2006, AJ, 131, 1163
Sundelius, B., Wahde, M., Lehto, H. J., & Valtonen, M. J. 1997, ApJ, 484, 180
Timmer, J., & Koenig, M. 1995, A&A, 300, 707
Valtonen, M., & Ciprini, S. 2012, MmSAI, 83, 219
van der Klis, M. 1988, in NATO Advanced Science Institutes (ASI) Series C Vol. 262, Timing Neutron Stars, ed. H. Ogelman & E. P. J. Van den Heuvel (Dordrecht: Kluwer), 27
van der Klis, M. 1989, ARA&A, 27, 517
Vaughan, S. 2005, A&A, 431, 391
Vaughan, S. 2010, MNRAS, 402, 307
Villata, M., & Raiteri, C. M. 1999, A&A, 347, 30
Welch, P. D. 1967, IEEE Transactions on Audio and Electroacoustics, 15, 70
Zerbi, F. M., Chincarini, G., Ghisellini, G., et al. 2004, Proc. SPIE, 5492, 1590
Zhang, B.-K., Zhao, X.-Y., Wang, C.-X., & Dai, B.-Z. 2014, RAA, 14, 933
Zhou, W.-X., & Sornette, D. 2002, IJMPC, 13, 137